Hindawi
International Journal of RF and Microwave Computer-Aided Engineering
Volume 2024, Article ID 4638443, 12 pages
https://doi.org/10.1155/2024/4638443

Research Article

Analyzing Three Types of Design Methods for 5G N41 Band Acoustic Wave Filters

Youna Jang[1] **and Dal Ahn**[2]

[1]*Department of ICT Convergence, Soonchunhyang University, Republic of Korea*
[2]*Department of Electrical Engineering, Soonchunhyang University, Republic of Korea*

Correspondence should be addressed to Dal Ahn; dahnkr@sch.ac.kr

Received 13 September 2023; Revised 4 December 2023; Accepted 15 December 2023; Published 13 January 2024

Academic Editor: Jin Xu

This paper presents three design methods for acoustic wave (AW) filters: the direct conversion design method, the slope parameter method, and the band edge fitting method (BEFM). Since the conventional BVD model consists only of lumped elements and has accuracy only near the resonance frequency, an NM-BVD model capable of broadband modeling is proposed in this paper and used to design the filter. In the proposed BEFM, a systematically optimal filter method is used to design the AW filter, and each AW resonator is tuned to the filter prototype value to meet the desired specifications. Thus, the filter design time and the number of resonators can be efficiently improved, and the filter design time can be reduced compared with the direct conversion and slope parameter methods commonly used in filter design. To demonstrate the effectiveness of these design methods, the proposed methods were used to design and fabricate an N41 filter using scandium-doped aluminum nitride (ScAlN) resonators. The broadband capabilities of the filter were verified using BEFM. The design, fabrication, and measurement of a broadband filter that meets the requirements of the 5G N41 frequency band centered at 2.593 GHz with a bandwidth of 196 MHz have verified the filter fabricated using the proposed design method. The insertion loss is less than -3 dB in the target band and more than 30 dB out of band. In summary, the proposed BEFM provides an efficient and accurate method for designing AW filters.

1. Introduction

The acoustic wave (AW) resonators find wide application in analog communications as RF filters, especially in RF front-end systems and cellular phones. The importance of AW resonators has grown due to their essential performance requirements for analog filters: low insertion loss, small size, and excellent selectivity. Synthesizing AW filters using AW resonators has been achieved through several methods [1–5]. Typically, in ladder-type AW filters [6–11], the resonant frequency of the series resonator and the antiresonant frequency of the parallel resonator are adjusted to align with the desired bandwidth's center frequency.

In ladder-type AW filters, the series resonator generates a resonant frequency within the passband of the filter. The antiresonant frequency of the parallel resonator is used to attenuate signals within the passband. The filter can achieve accurate filtering and high selectivity of signals within the desired frequency range by adjusting these frequencies to be close to the center frequency of the desired bandwidth. However, these methods are not effective in determining the minimum number of AW resonators necessary to achieve the desired attenuation response.

Chebyshev and elliptic filters can be created through the use of RLC resonators in order to attain optimal performance. The corresponding generalized filter functions are utilized to calculate the coefficients of both the numerator and denominator of the transfer function. Using the generalized filter functions, the coefficients of the numerator and denominator polynomials of the transfer function can also be calculated to synthesize Chebyshev and elliptic filters with RLC resonators [12, 13]. The problem of obtaining the poles and zeros in the complex plane is solved by the roots of the numerator and denominator. The pole-zero distribution

resulting from this process is used to synthesize and assess the filter's frequency response. There are two additional factors to consider when designing an AW filter. Firstly, the circuit topology must incorporate the fewest resonators possible. Secondly, the characteristics of every AW resonator require careful consideration. While certain synthesis methods [12–14] for Chebyshev/elliptic filters advocate for using the minimum number of resonators, the resulting parameter values may not be practical for real-world applications. For instance, the method could have inductance values up to 200 nH or capacitance values that are too low for the filter structure. It could also present challenges in filter fabrication when each resonator has a distinct coupling coefficient. While the impedance inverter method [15] provides a theoretical design approach, it is limited by the band response of the negative capacitance.

Therefore, a hybrid approach using transmission lines based on a coupling matrix [16] is used to design the BAW resonator, which has a limited coupling coefficient. In addition, the out-of-band and insertion loss results are not satisfactory despite using a 3rd-order filter design.

Three different AW filter design methods, namely, the direct conversion method, the slope parameter method, and the proposed band edge fitting method (BEFM), are presented in this paper. While these methods have been used previously for LC filter design, the proposed BEFM approach has been shown to be particularly effective in the design of the N41 wideband filter. As one of the key LTE bands, also included in the latest 5G NR standards, the N41 frequency band, which has been extensively studied [17], is of significant importance. In particular, the N41 band operates in close proximity to the Wi-Fi band (2400 MHz-2483 MHz). This requires the use of a highly selective filter to effectively meet the stringent coexistence requirements [18]. The N41 filter is broadband, and the design can only consist of AW resonators. Therefore, verification of the filter design is well suited for demonstration.

We also propose the newly modified Butterworth-Van Dyke (NM-BVD) model for accurate design in broadband. The proposed BEFM for 196 MHz bandwidth is applied to design the N41 filter. Through the fabrication results of the N41 filter, it is found that the proposed design method shows good performance with the minimum number of resonators while reducing the optimization time.

2. NM-BVD Model

A modified Butterworth-Van Dyke (mBVD) model of the AW resonator is commonly used to validate the electrical performance of the AW resonator [19]. The reactive elements of C_P, C_m, and L_m describe the basic model of the AW resonator, while the three resistors of R_s, R_p, and R_m model the electrical losses, perimeter losses, and bulk losses, as shown in Figure 1. However, the conventional mBVD model is limited in its ability to accurately predict the magnitude of electrical properties only in the vicinity of the resonant and antiresonant frequency ranges. This is due to the use of lumped elements. However, for frequencies outside these ranges, phase discrepancies with actual measurement results may occur. To overcome this limitation, we propose a new modified Butterworth-Van Dyke (NM-BVD) model. This model provides improved simulation accuracy for broadband applications. In the NM-BVD model, electrical lengths are added to improve the accuracy of the filter design. They reduce out-of-resonance band errors and lead to improvements in phase differences.

The fabricated SnP model and the NM-BVD model structure of the conventional BVD model with electrical lengths are shown in Figures 1(a) and 1(b). The comparative simulation results of the measured resonator, the conventional BVD model, and the proposed BVD model are shown in Figures 2(a) and 2(b). The measured series resonator has a resonant frequency of 2.653 GHz and an antiresonant frequency of 2.771 GHz, using a 12% coupling coefficient ($R_s = 0.52\,\Omega$, $R_p = 0.22\,\Omega$, and $R_m = 0.146\,\Omega$). While the magnitude comparison results are similar to the measurement result, the phase results show differences in the electrical characteristics at deviations from the resonance frequency in the case of the conventional model. The comparison results show that the proposed NM-BVD model improves the phase performance by more than 1.3 within the 2-3 GHz band. This means that the difference between the designed circuit and the fabricated circuit increases when only the conventional BVD model with only lumped parameters is used for filter design.

In particular, the electrical properties of the NM-BVD model are similar to those of the conventional BVD model near the resonant frequency band, since the lumped elements are targeted only near the resonant frequency and antiresonant frequency regions. However, in other frequency bands, the differences between the two models can become significant. This can lead to significant differences in the design of broadband filters. Therefore, the NM-BVD model is an accurate model for circuit simulation that combines lumped and distributed elements. It helps reduce errors not only in the passband but also in the attenuation band.

3. Design Methods

Previous studies [6–11] have used a ladder-type network with an in-line topology to synthesize acoustic wave filters, as shown in Figure 3. In this design approach, the resonant frequency of the series resonator and the antiresonant frequency of the shunt resonator are usually designed to match the center frequency of the target band. However, it can be difficult to implement the minimum number of resonators required to meet the design specifications using this method. In addition, optimizing the performance of the filter to meet the design specifications can be time-consuming compared to a systematic design approach. Therefore, three types of methods are proposed in this chapter for a systematic approach to filter design: the direct conversion method, the slope parameter method, and the band edge fitting method.

3.1. Direct Conversion Method. The term "low-pass filter" is generally used to describe a filter in which the element values are normalized so that the source resistance or conductance is equal to one ($g_0 = 1$) and the cutoff angular frequency is normalized to unity ($\omega_c = 1$ rad/s). This definition is relevant

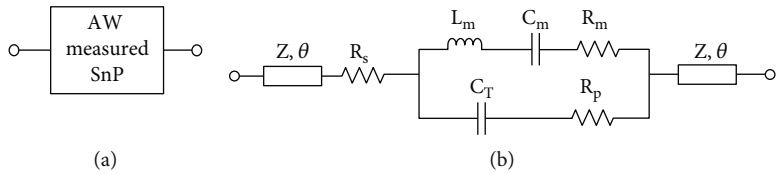

FIGURE 1: (a) Fabricated data symbol (SnP). (b) Proposed NM-BVD model of AW.

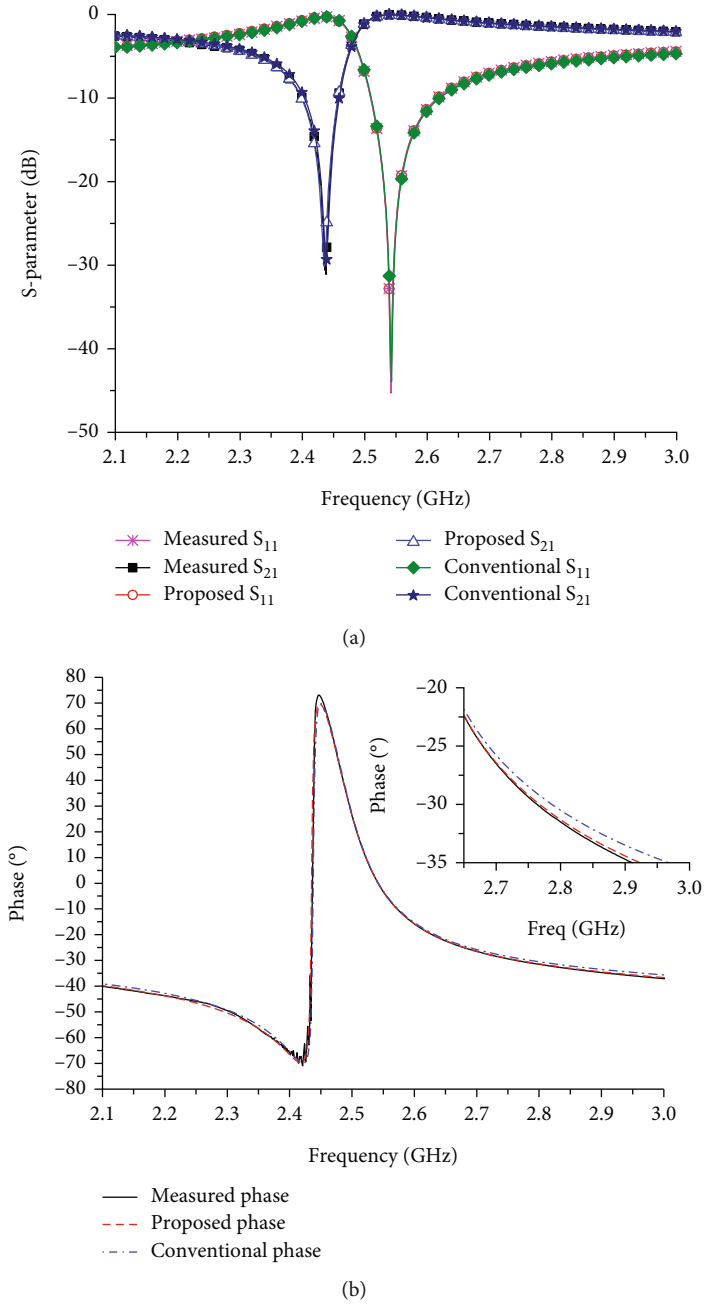

FIGURE 2: Comparison results between measurement and modeling: (a) magnitude and (b) phase response.

to RF and microwave filter design techniques. Many practical filter designs involve transformations of frequency and elements. This chapter uses this notion of a low-pass filter, as shown in Figure 3(a).

The low-pass prototype response is transformed into a band-pass response using a frequency-mapping function, and the lumped elements of the AW resonator are converted from the low-pass prototype, which is the direct conversion

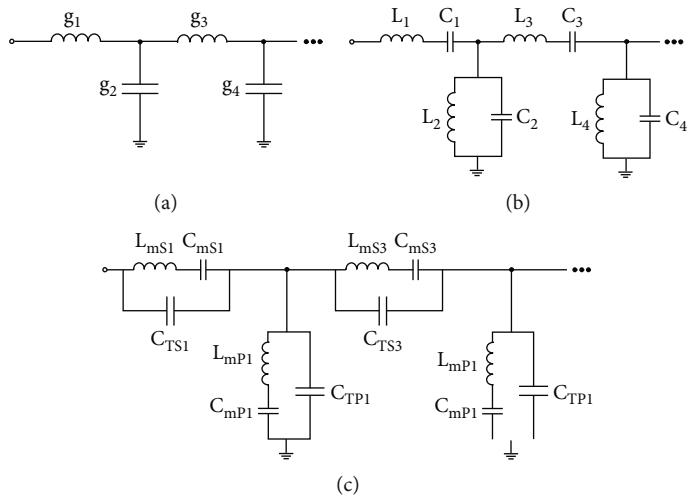

Figure 3: AW filter design using 1 port resonator and mapping function method: (a) low-pass filter structure; (b) band-pass filter direct conversion structure; (c) band-pass filter to AW filter conversion structure with mapping function.

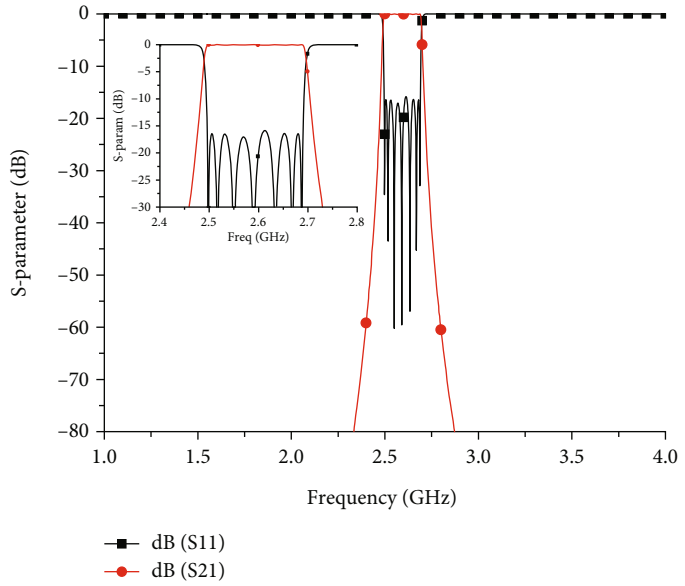

Figure 4: Simulation results of the N41 filter using direct conversion method.

Table 1: Parameter values of direct conversion method for N41 filter.

Resonators	L_m (nH)	C_m (pF)	C_T (pF)
$P_1 = P_7$	0.19	52007.68	19.37
$P_3 = P_5$	0.109	92320.13	34.387
$S_2 = S_4$	58.34	0.065	0.0046
S_3	64.51	0.058	0.004

method [20, 21], as shown in Figure 3(b). The resonant and antiresonant frequencies of each resonator are determined based on the lossless resonators. The reactance component of the series resonator is defined by the parameters of the equivalent resonant circuit described in

$$Z_{\text{in}} = jX_s = j\frac{\omega^2 L_{\text{ms}} C_{\text{ms}} - 1}{\omega C_{\text{ms}} - \omega C_{\text{Ts}}(\omega^2 L_{\text{ms}} C_{\text{ms}} - 1)}. \quad (1)$$

The resonant frequency of the series arm is an angular resonant frequency (ω_{rs}) at which the reactance term is zero, while the antiresonant frequency of the series arm is an angular antiresonant frequency (ω_{ars}) at which the reactance term is infinite as

$$\omega_{\text{rs}}^2 = \frac{1}{L_{\text{ms}} C_{\text{ms}}}, \qquad f_{\text{rs}} = \frac{1}{2\pi\sqrt{L_{\text{ms}} C_{\text{ms}}}}, \quad (2)$$

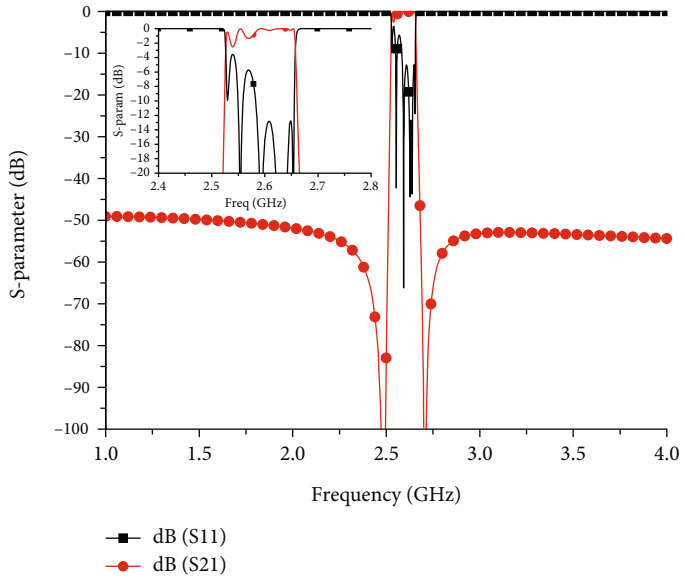

Figure 5: Simulation results of the N41 filter using slope parameter method.

Table 2: Parameter values of slope parameter method for N41 filter.

Resonators	L_m (nH)	C_m (pF)	C_T (pF)
$P_1 = P_7$	22.4	0.183	2.088
$P_3 = P_5$	10.01	0.409	4.67
$S_2 = S_4$	57.34	0.065	0.733
S_3	66.87	0.056	0.628

$$\omega_{\text{ars}}^2 = \omega_{\text{rs}}^2\left(1 + \frac{C_{\text{ms}}}{C_{\text{Ts}}}\right),$$
$$f_{\text{ars}} = f_{\text{rs}}\sqrt{1 + \frac{C_{\text{ms}}}{C_{\text{Ts}}}}. \tag{3}$$

The susceptance part of the parallel resonator is also defined as follows:

$$Y_{\text{in}} = jB_p = j\frac{\omega C_{\text{Tp}}\left(\omega^2 L_{\text{mp}} C_{\text{mp}} - 1\right) - \omega C_{\text{mp}}}{\omega^2 L_{\text{mp}} C_{\text{mp}} - 1}. \tag{4}$$

The resonant frequency of the parallel resonator is an angular resonant frequency (ω_{rp}) at which the susceptance term is zero, while the antiresonant frequency of the parallel arm is an angular antiresonant frequency (ω_{arp}) as

$$\omega_{\text{rp}}^2 = \frac{1}{L_{\text{mp}} C_{\text{mp}}},$$
$$f_{\text{rp}} = \frac{1}{2\pi\sqrt{L_{\text{mp}} C_{\text{mp}}}}, \tag{5}$$

$$\omega_{\text{arp}}^2 = \omega_{\text{rp}}^2\left(1 + \frac{C_{\text{mp}}}{C_{\text{Tp}}}\right),$$
$$f_{\text{arp}} = f_{\text{rp}}\sqrt{1 + \frac{C_{\text{mp}}}{C_{\text{Tp}}}}. \tag{6}$$

The center frequency of the desired band is used to determine the resonant frequency of the series arm and the antiresonant frequency of the parallel arm, which together form the band-pass filter. The AW filter is also transformed from a low-pass filter to a band-pass filter using a frequency-mapping function similar to that used for conventional filters. The frequency-mapping functions for the series and parallel resonators are expressed as follows:

$$\frac{\omega'}{\omega'_1} = \frac{\omega^2 - \omega_{\text{rs}}^2}{\omega\left(\omega_{\text{ars}}^2 - \omega^2\right)} \cdot \frac{\omega_2\left(\omega_{\text{ars}}^2 - \omega_2^2\right)}{\omega_2^2 - \omega_{\text{rs}}^2}, \tag{7}$$

$$\frac{\omega'}{\omega'_1} = \frac{\omega\left(\omega^2 - \omega_{\text{arp}}^2\right)}{\omega^2 - \omega_{\text{rp}}^2} \cdot \frac{\omega_{\text{rp}}^2 - \omega_1^2}{\omega_1\left(\omega_1^2 - \omega_{\text{arp}}^2\right)}. \tag{8}$$

These equations are for mapping the low-pass prototype filter response to the corresponding band-pass filter response. ω' and ω'_1 are for the prototype filter responses

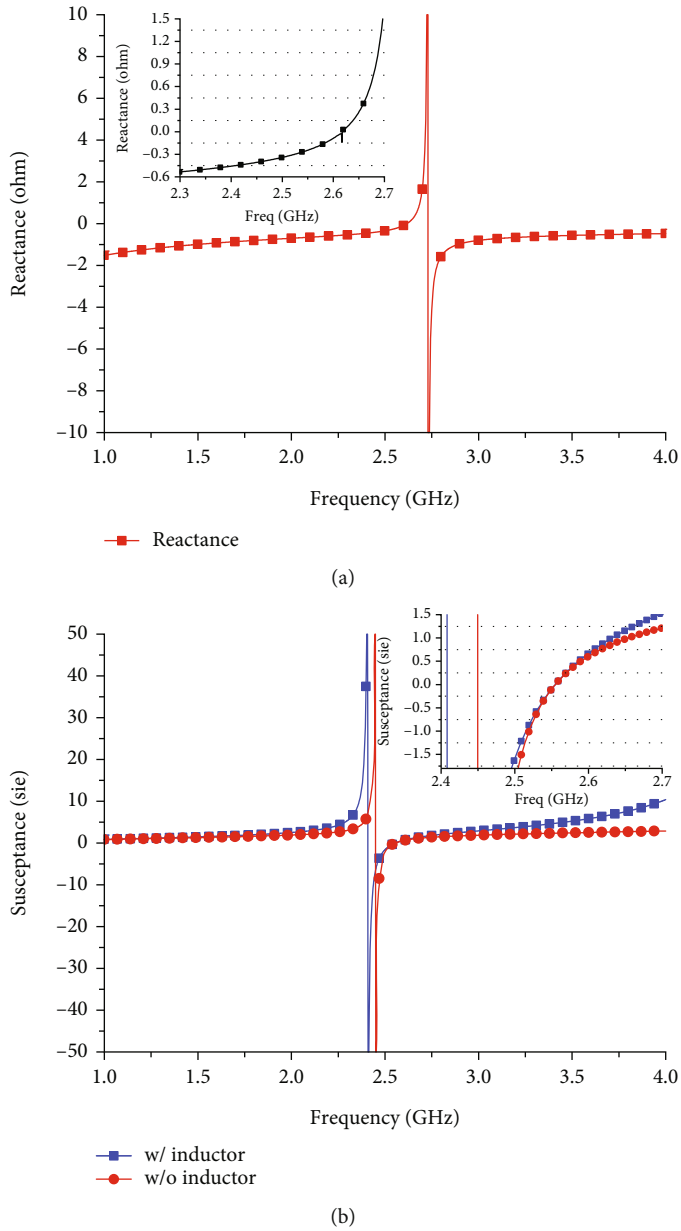

FIGURE 6: Band edge fitting method: (a) fitting method for series resonator and (b) fitting method for parallel resonator with or without inductor.

in [22]. Applying the mapping functions (7) and (8), the band-pass filter is obtained as shown in Figure 3. Thus, the parameter values of the series and parallel equivalent circuit models are given by the following equations:

$$C_{\mathrm{Ts}} = \frac{\omega^2 - \omega_{\mathrm{rs}}^2}{\omega_2\left(\omega_{\mathrm{ars}}^2 - \omega_2^2\right) g_i Z_0},$$
$$C_{\mathrm{ms}} = C_{\mathrm{Ts}}\left(\frac{\omega_{\mathrm{ars}}^2}{\omega_{\mathrm{rs}}^2} - 1\right), \tag{9}$$
$$L_{\mathrm{ms}} = \frac{1}{C_{\mathrm{ms}}\omega_{\mathrm{rs}}^2},$$

$$C_{\mathrm{Tp}} = \frac{\left(\omega_{\mathrm{rp}}^2 - \omega_1^2\right) g_i}{\omega_1\left(\omega_1^2 - \omega_{\mathrm{arp}}^2\right) Z_0},$$
$$C_{\mathrm{mp}} = C_{\mathrm{Tp}}\left(\frac{\omega_{\mathrm{arp}}^2}{\omega_{\mathrm{rp}}^2} - 1\right), \tag{10}$$
$$L_{\mathrm{mp}} = \frac{1}{C_{\mathrm{mp}}\omega_{\mathrm{arp}}^2}.$$

Z_0 is the port impedance, typically 50 ohms. The g_i are the prototype filter element values from [22].

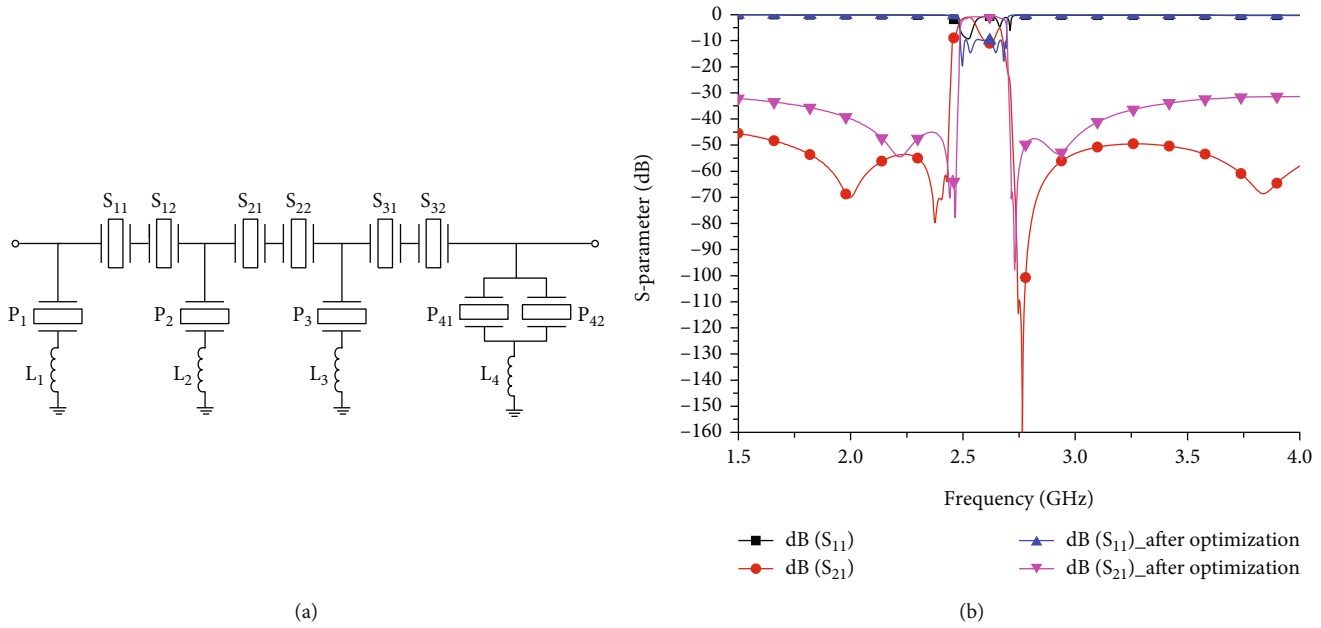

(a) (b)

FIGURE 7: (a) Fitting method for series resonator. (b) Simulation results of before and after optimization using proposed method.

In general, as shown in Figure 3(c), a ladder-type filter typically uses a series and parallel arrangement of AW resonators to achieve a desired frequency response. By combining the resonant and antiresonant frequencies of each series and parallel resonator, it is possible to achieve the passband and attenuation in the stop band. The elliptic prototype value was not used in this study. The addition of a shunt inductor was sufficient to achieve the desired band response. The simulation results of the N41 filter with a BW of 2.496-2.69 GHz using the direct conversion method are shown in Figure 4. The simulation results show that the return loss is 16.4 dB. This is in good agreement with the Chebyshev return loss at 0.1 dB ripple. Based on the parallel resonator of the ladder structure, the parameter values of Figure 4 are shown in Table 1. However, some of the parameter values are too high or too low, so it is difficult to implement the acoustic wave resonator.

3.2. Slope Parameter for Narrow Bandwidth. In this section, the slope parameter method is used to design AW filters. In practice, narrowband filters usually approximate the reactances or susceptances of lumped resonators only near the resonance frequency. To obtain the reactance/susceptance and the reactance/susceptance slope of the AW resonator, the corresponding lumped resonator values are transformed from the low-pass prototype values at the center frequency of the target band. These two quantities, called the reactance slope parameter and susceptance slope parameter, respectively, are referred to [20]. The reactance slope parameter for resonators with zero reactance at the center frequency ω_0 is defined as (10), where g_k is the generic term for the low-pass prototype elements in the element transformation [20]. The resonator reactances using (1) in the AW equivalent circuit, when ω is ω_s, are determined by the slope parameter equation as follows:

$$\left.\frac{dX_{\text{in}}}{d\omega}\right|_{\omega=\omega_0} = \frac{2g_kZ_0}{\varpi\omega_0}, \text{ where } \varpi = \frac{\omega_2-\omega_1}{\omega_0}, \tag{11}$$

$$\left.\frac{dX_{\text{in}}}{d\omega}\right|_{\omega=\omega_s} = -\frac{2}{\omega_s^2\left(C_s+C_p\right)\left[\left(\omega_s/\omega_p\right)^2-1\right]}. \tag{12}$$

In the dual case, the susceptance slope parameter for resonators is made equal to its corresponding value for the parallel lumped resonator, at $\omega = \omega_0$, by

$$\left.\frac{dB_{\text{in}}}{d\omega}\right|_{\omega=\omega_0} = \frac{2g_k}{\varpi\omega_0Z_0}, \text{ where } \varpi = \frac{\omega_2-\omega_1}{\omega_0}. \tag{13}$$

The susceptance value of the AW resonator using (4) is determined by equating the slope parameters as

$$\left.\frac{dB_{\text{in}}}{d\omega}\right|_{\omega=\omega_p} = \frac{2\left(C_s+C_p\right)}{\left(\omega_p/\omega_s\right)^2-1}. \tag{14}$$

The AW resonator resonant and antiresonant frequencies are calculated to position the series resonator resonant frequency and the parallel resonator antiresonant frequency near the center frequency of the desired passband. In practice, slope parameters are often used to approximate the reactances and susceptances of the AW equivalent circuit around the resonant frequencies ω_s and ω_p.

The slope parameter method is a dependable design approach that ensures a precise match for the parallel antiresonant and series resonant frequencies. The results in Figure 5 display the fit starting from the parallel resonator in the 7th-order filter. Table 2 confirms that the assigned parameter values for each resonator are well suited for their

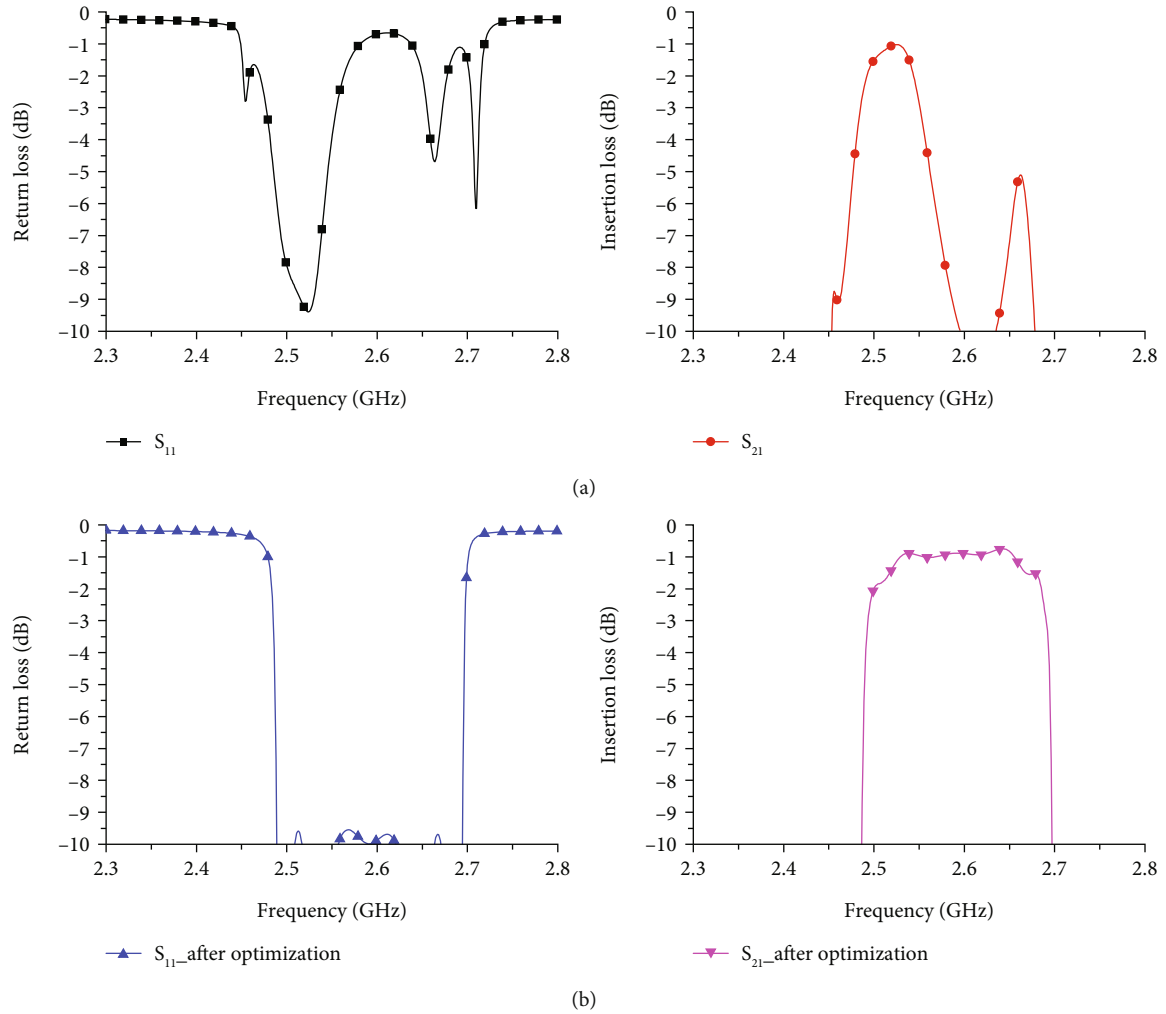

FIGURE 8: Insertion loss graphs of before and after optimization in Figure 7: (a) before optimization results and (b) after optimization results of S11 and S21.

implementation. However, the use of a 12% coupling coefficient for the N41 filter in Figure 5 creates a narrower bandwidth than specified. This result, which is solely from the design calculation process and does not involve optimization, is best suited for narrow bandwidths of approximately less than 60 MHz compared to the target band. The slope parameter method is generally appropriate for such narrow bandwidths.

3.3. Band Edge Fitting Method for Wide Band. The slope parameter method is effective for narrowband filters but has limitations regarding broadband filters. To widen the target bandwidth, it is essential to adjust the normalized reactance or susceptance value to the filter prototype value, g_k, instead of modifying the slope of the reactance curve, as explained in

$$\left.\frac{\mathrm{Im}\,(Z_{12})}{Z_0}\right|_{\omega=\omega_2} = \left.\frac{\omega^2 L_s C_s - 1}{\omega C_s - \omega C_p(\omega^2 L_s C_s - 1)}\frac{1}{Z_0}\right|_{\omega=\omega_2} = g_k, \tag{15}$$

TABLE 3: Optimized NM-BVD parameters for a N41 AW filter using band edge fitting method.

NM-BVD elements	L_m (nH)	C_m (pF)	C_T (pF)
P_1	51.57	0.08	0.91
P_2	28.04	0.146	1.672
P_3	29.22	0.14	1.62
$P_{41} = P_{42}$	88.09	0.04	0.297
$S_{11} = S_{12}$	23.17	0.159	1.76
$S_{21} = S_{22}$	19.28	0.194	2.24
$S_{31} = S_{32}$	22.42	0.165	1.792

$$\left.\frac{\mathrm{Im}\,(Z_{12})}{Z_0}\right|_{\omega=\omega_0} \approx 0. \tag{16}$$

The normalized reactance of the series resonator, Im (z_{12}), often has a sharp slope close to the band edge frequency at ω_2, as shown in Figure 6(a). On the other hand, in the dual case, the normalized susceptance of the parallel

Table 4: External inductance values for a N41 AW filter using band edge fitting method.

	L_1 (nH)	L_2 (nH)	L_3 (nH)	L_4 (nH)
External	0.69	0.78	0.53	2.74

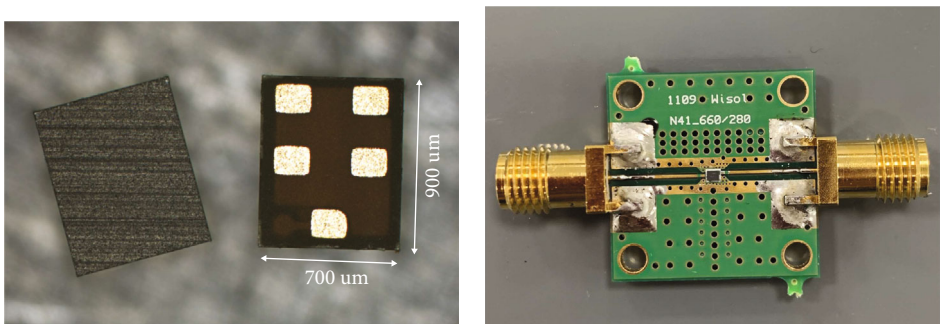

(a) (b)

Figure 9: (a) Footprint and top view image of N41 filter chip. (b) Fabricated chip on the PCB using SMA connector.

resonator, Im (y_{11}), forms the slope close to the band edge frequency at ω_1, leading to

$$\left.\frac{\mathrm{Im}\,(Y_{11})}{Y_0}\right|_{\omega=\omega_1} = \left.\frac{\omega C_{\mathrm{Tp}}\left(\omega^2 L_m C_m - 1\right) - \omega C_m}{\omega^2 L_m C_m - 1}\frac{1}{Y_0}\right|_{\omega=\omega_1} = -g_k, \tag{17}$$

$$\left.\frac{\mathrm{Im}\,(Y_{11})}{Y_0}\right|_{\omega=\omega_0} \approx 0. \tag{18}$$

In the series resonator, the electrical response slope undergoes a gradual change at a lower frequency than ω_2. The parallel resonator works similarly to the dual case. Thus, the value of the reactance or susceptance is set to zero as much as possible when ω is ω_0, as expressed in (16) and (18). However, due to the difference in slope, the center frequency for the reactance or susceptance value will be slightly different from zero. In general, given the target band, the coupling coefficient of the AW resonator is expressed by the following equation [23, 24].

$$k_{\mathrm{eff}}^2 = \frac{\pi f_s}{2f_p}\cot\left(\frac{\pi f_s}{2f_p}\right), \tag{19}$$

which is directly related to the frequency separation between the resonant frequency and the antiresonant frequency.

4. Design of N41 AW Filter

To showcase the efficacy of the proposed band edge fitting method (BEFM) in designing AW filters, this section presents an instance of its implementation for a N41 band specification (2.496-2.69 GHz). The center frequency is set to 2.593 GHz. First, the BAW resonator was modeled using the proposed NM-BVD model. To achieve the target bandwidth of 194 MHz, a BAW resonator with a coupling coefficient of 12% was designed using BEFM. To meet the attenuation specifications, a 7th-order filter with prototype values that matched the Chebyshev response at 0.01 dB ripple was required.

The Chebyshev response values were $g1 = g7 = 0.7969$, $g2 = g6 = 1.3924$, $g3 = g5 = 1.7481$, and $g4 = 1.6331$. When designing the filter using parallel resonators, the susceptance value of the first parallel resonator was adjusted to $g1$ as explained in Section 5. The reactance value of the second series resonator was then adjusted to be close to ±1.3924 at the higher cutoff frequency of the N41 filter, as shown in Figure 6(a). However, the third parallel resonator's susceptance value did not fit well to ±1.7481. Therefore, a shunt inductor was added to the parallel resonator. The normalized susceptance value of the lower frequency in the band edge was well matched to ±1.7481, as shown in Figure 6(b). The added shunt inductor (0.85 nH) not only helped to fit the prototype value but also set the transmission zero (TZ) for the target specifications.

The 7th-order resonators of the N41 filter were modeled using the Chebyshev prototype, and the first results of the multiresonator modeling are shown in Figures 7 and 8. The design method used is based on BEFM. Although the modeling results need improvement in terms of insertion loss, the simulation results show a good attenuation response. By using BEFM, filter designers can apply an accurate design method that reduces the time required for simulation and optimization. Tables 3 and 4 show the optimized NM-BVD parameter values for the N41 filter.

5. Fabrication and Measurement Results

To validate the effectiveness of the proposed filter design method, the N41 filter was fabricated and tested. Figures 9(a) and 9(b) show the chip image of the fabricated N41 filter and the filter mounted on an FR6 printed circuit board (PCB) with a dielectric constant of 2.46, respectively. A

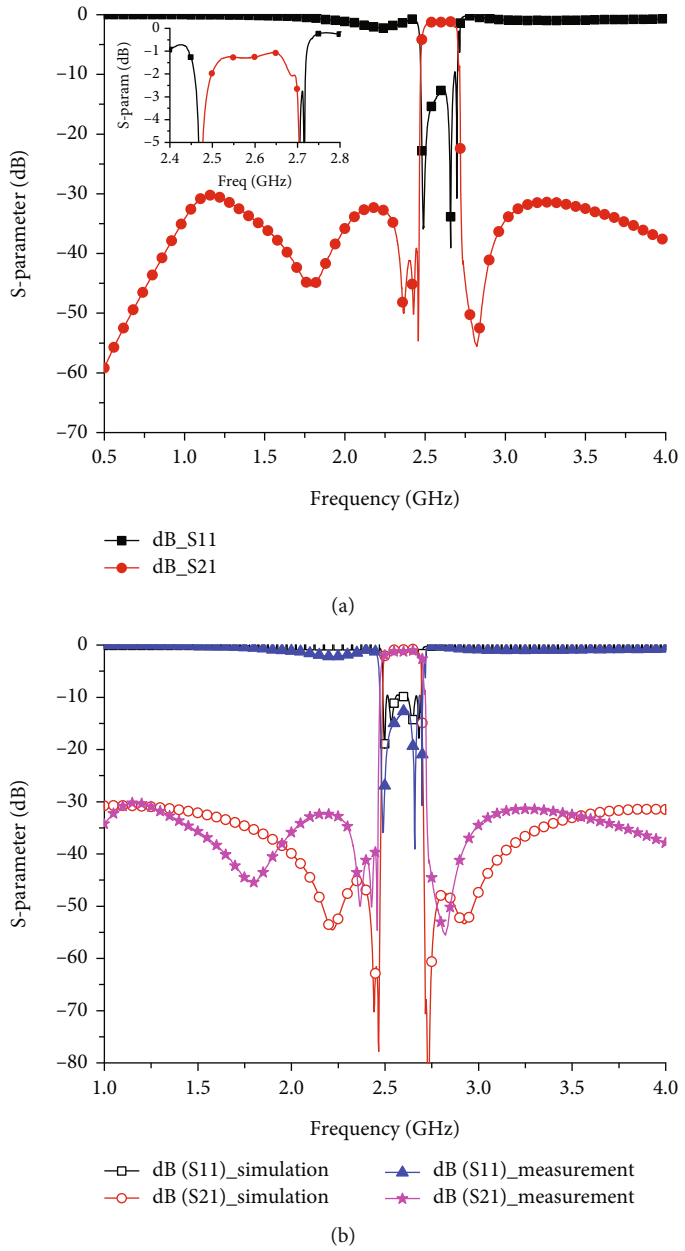

Figure 10: (a) Fabricated results of the proposed N41 filter. (b) Comparison results of simulation and measurement.

scandium-doped aluminum nitride (ScAlN) resonator with a coupling coefficient of 12% supplied by Wisol Inc. The Sc content is 12%, the piezo thickness is 600 nm, and the thickness of the top and bottom electrodes is 209–265 nm. The filter layout was designed with a size of $900 \times 700\ \mu m^2$. SMA connectors were soldered to the PCB substrate to allow measurement of the fabricated chip.

Resonators were fabricated using 6-inch high-resistivity silicon (HRS) to achieve the target frequencies of the series and shunt resonators with low loss and high attenuation. The results of the fabricated N41 filter are shown in Figure 10, which shows that the attenuation is less than 30 dB except in the passband, and the attenuation results are greater than 40 dB in the 2.3–2.473 GHz range.

6. Conclusion

In this paper, we present three design methods for acoustic wave (AW) filters, namely, the direct conversion method, the slope parameter method, and the band edge fitting method (BEFM). Additionally, we propose a newly modified Butterworth-Van Dyke (NM-BVD) model for the equivalent circuit by modifying the conventional BVD model to match the resonator measurement. This equivalent circuit is then employed for the circuit design. The direct conversion method and the slope parameter technique are widely recognized as effective filter design methods, but they have limitations in achieving practical, implementable inductance or capacitance values and in achieving a broadband design.

The BEFM is proposed as a promising alternative to these methods. The proposed BEFM matches filter prototype values to meet specific requirements, leading to enhanced efficiency in the time required for filter design and a decreased need for resonators. An N41 filter was specifically designed and fabricated using scandium-doped aluminum nitride (ScAlN) resonators. To establish its effectiveness, the filter's broadband capabilities were verified via the BEFM. The filter manufactured by utilizing the recommended approach effectively fulfilled the specifications of the 5G N41 frequency band, positioned at 2.593 GHz with a bandwidth of 196 MHz. The filter showed an insertion loss of under -2.1 dB within the specified frequency range and over 30 dB out-of-band attenuation. The BEFM offers an effective and precise approach for designing acoustic wave (AW) filters. Its effectiveness is demonstrated through the design, fabrication, and measurement of a wideband filter for the 5G N41 frequency band.

Data Availability

All data generated or analyzed during this study are included in this published article.

Conflicts of Interest

The authors declare that there are no conflicts of interest regarding the publication of this paper.

Authors' Contributions

All listed authors (Youna Jang and Dal Ahn) made substantial scientific contributions to the research in the paper, approved the claims in the paper, and agreed to be authors.

Acknowledgments

We are very grateful to Wisol Co., Ltd. for fabricating the filter chip for this manuscript. This research was supported by the MSIT (Ministry of Science and ICT), Korea, under the ICAN (ICT Challenge and Advanced Network of HRD) program (IITP-2024-2020-0-01832) supervised by the IITP (Institute of Information & Communications Technology Planning & Evaluation) and Soonchunhyang University Research Fund.

References

[1] S. V. Krishnaswamy, J. Rosenbaum, S. Horwitz, C. Vale, and R. A. Moore, "Compact FBAR filters offer low-loss performance," *Microwaves & RF*, vol. 30, pp. 127–136, 1991.

[2] F. M. Pitschi, J. E. Kiwitt, R. D. Koch, B. Bader, K. Wagner, and R. Weigel, "High performance microwave acoustic components for mobile radios," in *2009 IEEE International Ultrasonics Symposium*, pp. 1–10, Rome, Italy, September 2009.

[3] T. Bauer, C. Eggs, K. Wagner, and P. Hagn, "A bright outlook for acoustic filtering: a new generation of very low-profile SAW, TC SAW, and BAW devices for module integration," *IEEE Microwave Magazine*, vol. 16, no. 7, pp. 73–81, 2015.

[4] S. Mahon, "The 5G effect on RF filter technologies," *IEEE Transactions on Semiconductor Manufacturing*, vol. 30, no. 4, pp. 494–499, 2017.

[5] R. Ruby, "A snapshot in time: the future in filters for cell phones," *IEEE Microwave Magazine*, vol. 16, no. 7, pp. 46–59, 2015.

[6] P. Warder and A. Link, "Golden age for filter design: innovative and proven approaches for acoustic filter duplexer and multiplexer design," *IEEE Microwave Magazine*, vol. 16, no. 7, pp. 60–72, 2015.

[7] C. C. W. Ruppel, "Acoustic wave filter technology–a review," *IEEE Transactions on Ultrasonics, Ferroelectrics, and Frequency Control*, vol. 64, no. 9, pp. 1390–1400, 2017.

[8] A. Giménez, J. Verdú, and P. De Paco Sánchez, "General synthesis methodology for the design of acoustic wave ladder filters and duplexers," *IEEE Access*, vol. 6, pp. 47969–47979, 2018.

[9] Ó. Menéndez, P. de Paco, R. Villarino, and J. Parron, "Closed-form expressions for the design of ladder-type FBAR filters," *IEEE Microwave and Wireless Components Letters*, vol. 16, no. 12, pp. 657–659, 2006.

[10] S. Giraud, S. Bila, M. Chatras, D. Cros, and M. Aubourg, "Bulk acoustic wave filters synthesis and optimization for multi-standard communication terminals," *IEEE Transactions on Ultrasonics, Ferroelectrics, and Frequency Control*, vol. 57, no. 1, pp. 52–58, 2010.

[11] M. Ylilammi, J. Ella, M. Partanen, and J. Kaitila, "Thin film bulk acoustic wave filter," *IEEE Transactions on Ultrasonics, Ferroelectrics, and Frequency Control*, vol. 49, no. 4, pp. 535–539, 2002.

[12] S.-Y. Tseng and R.-B. Wu, "Synthesis of Chebyshev/elliptic filters using minimum acoustic wave resonators," *IEEE Access*, vol. 7, pp. 103456–103462, 2019.

[13] S.-Y. Tseng, C.-C. Hsiao, and R.-B. Wu, "Synthesis and realization of Chebyshev filters based on constant electromechanical coupling coefficient acoustic wave resonators," in *2020 IEEE/MTT-S International Microwave Symposium (IMS)*, pp. 257–260, Los Angeles, CA, USA, August 2020.

[14] E. Guerrero, P. Silveira, J. Verdu, Y. Yang, S. Gong, and P. de Paco, "A synthesis approach to acoustic wave ladder filters and duplexers starting with shunt resonator," *IEEE Transactions on Microwave Theory and Techniques*, vol. 69, no. 1, pp. 629–638, 2021.

[15] Ó. Menéndez, P. de Paco, J. Gemio, J. Verdú, and E. Corrales, "Methodology for designing microwave acoustic filters with Butterworth/Chebyshev response," *International Journal of Microwave and Wireless Technologies*, vol. 1, no. 1, pp. 11–18, 2009.

[16] G. Ariturk, N. R. Almuqati, Y. Yu, E. T.-T. Yen, A. Fruehling, and H. H. Sigmarsson, "Wideband hybrid acoustic-electromagnetic filters with prescribed Chebyshev functions," in *2022 IEEE/MTT-S International Microwave Symposium - IMS 2022*, pp. 887–890, Denver, CO, USA, June 2022.

[17] S. Kreuzer, A. Volatier, and G. Fattinger, "Full band 41 filter with high Wi-Fi rejection - design and manufacturing challenges," in *2015 IEEE International Ultrasonics Symposium (IUS)*, pp. 1–4, Taipei, Taiwan, October 2015.

[18] L. Jia, Y. Gao, C. Han, and J. Lu, "Design of a bulk acoustic wave filter in the WiFi band," *High Power Laser Science and Engineering*, vol. 29, no. 10, pp. 111–116, 2017.

[19] J. D. Larson, P. D. Bradley, S. Wartenberg, and R. C. Ruby, "Modified Butterworth-Van Dyke circuit for FBAR resonators

and automated measurement system," in *2000 IEEE Ultrasonics Symposium. Proceedings. An International Symposium (Cat. No.00CH37121)*, vol. 1, pp. 863–868, San Juan, PR, USA, October 2000.

[20] J.-S. Hong and M. J. Lancaster, *Microstrip Filters for RF/Microwave Applications*, Wiley, New York, 2nd edition, 2011.

[21] D. M. Pozar, *Microwave Engineering*, Wiley, New York, 3rd edition, 2009.

[22] G. Matthaei, L. Young, and E. M. T. Jones, *Microwave Filters, Impedance-Matching Networks and Coupling Structures*, Artech House Inc., Norwood, MA, 1980.

[23] J. A. Verdú Tirado, *Bulk Acoustic Wave Resonators and their Application to Microwave Devices*, Ph. D. dissertation, Universitat Autónoma de Barcelona, 2010.

[24] K. Y. Hashimoto, *RF Bulk Acoustic Wave Filers for Communications*, 2009, Artech House.